

A UNIFIED APPROACH TO MODEL PLANAR MULTILAYERED STRUCTURES WITH LATERAL PERFECT ELECTRIC/MAGNETIC AND PERIODIC BOUNDARY CONDITIONS

Pedro Crespo-Valero, Ivica Stevanović, and Juan R. Mosig

Laboratory of Electromagnetics and Acoustics (LEMA), École Polytechnique Fédérale de Lausanne (EPFL),
ELB-Station 11, CH-1015 Lausanne, Switzerland
{Pedro.CrespoValero, Ivica.Stevanovic, Juan.Mosig}@epfl.ch

ABSTRACT

This communication proposes a simple approach to model planar multilayered structures based on an Integral Equation technique. This method is applicable to a wide range of practical boundary conditions and basis functions while keeping a simple formulation in all cases. The technique is based on the modal representation of the Green's function in a laterally bounded media (e.g. waveguides or periodic structures) and reduces the surface integrals to simple line integrals over contour of the basis function's domain. The final formulation presents important advantages due to its generality, simplicity and efficiency.

Key words: Integral Equation, Green's Function, Method of Moments, Multilayer, Periodic Structure, Waveguide.

1. INTRODUCTION

Planar structures include many different geometries, ranging from cavity-backed microstrip antennas, to frequency-selective surfaces and photonic band-gap materials. In all of them, the presence of planar dielectric layers, metallic/slot surfaces and laterally bounding conditions is a common denominator. Therefore, any of the structures is represented by the generic electromagnetic (EM) problem depicted in Fig. 1.

From the point of view of mathematical and numerical modeling, one of the most successful approaches, providing a general framework for this type of structures, is the Integral Equation (IE) model combined with a discretization procedure like the Galerkin-Method of Moments (MoM) [1]. Essential to the IE-MoM approach is the knowledge of the pertinent Green's functions (GF).

For this problem, the formulation of the GF can consider the effect of the lateral boundaries and the multilayered media. Using the equivalence principle [2], the remaining elements embedded in the media, namely the planar

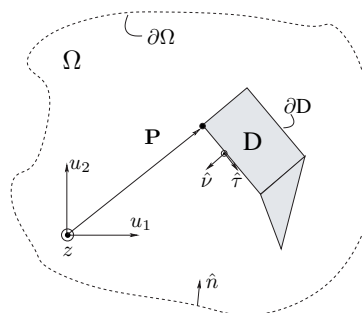


Figure 1. Representation of a generic cross-section of a laterally bounded planar-multilayered structure. The planar surfaces D represent electric/magnetic sources enclosed by a boundary $\partial\Omega$.

metallizations and slots, can be replaced by equivalent sources.

At this point, the election of basis functions to expand the sources or the type of BCs would traditionally require different formulations of the problem. Nevertheless, it will be demonstrated that it is possible to follow a unique strategy for a wide variety of practical basis functions and BCs.

The basic idea of this technique is in that the GF of the structure in Fig. 1 can always be formulated as a series expansion of modal functions satisfying a particular BC in the contour $\partial\Omega$. After application of the MoM, the series terms are transformed into integrals between modal and basis functions pairs over a surface domain D . These integrals can be further simplified by imposing a weak condition (almost universally used for this type of problems) on the basis functions.

The reduced complexity of the final formulation allows the specialization of the problem to a particular BC or basis function election with minor changes. Moreover, for practical BCs and basis functions, the integral expressions have analytical solutions, resulting in very efficient numerical algorithms. It also allows an easy check of

the numerical stability and convergence of the algorithms as well as a considerable reduction of the computer code needed for the implementation of different cases.

2. IE-MOM FORMULATION

A system of coupled IEs is obtained by imposing boundary conditions on the electric and magnetic equivalent surfaces embedded in the bounded-multilayered media as represented in Fig. 1. These sources are then expanded with pre-defined basis functions on domains D_k as

$$\mathbf{J}_Q(\mathbf{r}') = \sum_k \alpha_{Qk} \mathbf{f}_{Qk}(\mathbf{r}'), \quad k = 1, \dots, N_Q \quad (1)$$

where the source index $Q = E$ for a horizontal *electric* source or $Q = H$ for a horizontal *magnetic* source. In the same expression, α_{Qk} are the unknown coefficients in the expansion of the currents and \mathbf{f}_{Qk} are *irrotational* and *constant divergence* basis functions defined on electric ($Q = E$) or magnetic ($Q = H$) surfaces. This condition on the basis function is not very restrictive since it comprises most of the functions generally used in this kind of problems.

On the other hand, the GF for a multilayered structure, embedded into a given lateral boundary condition (BC), can be represented by means of an infinite series expansion

$$\vec{\mathbf{G}}_{PQ}(\mathbf{r}|\mathbf{r}') = \sum_i \tilde{G}_{P_i}(z, z') \mathbf{p}_i(x, y) \mathbf{q}_i^*(x', y'), \quad (2)$$

where the primed and unprimed coordinate refer to source and observer positions, respectively. Each term of this series contains two main components identifying the BCs encountered in the lateral and longitudinal directions. The first one embraces two eigenfunctions (or modal functions), denoted with $\{\mathbf{p}_i, \mathbf{q}_i\}$, satisfying the lateral BCs and evaluated in source and observer points. The second component \tilde{G}_{P_i} is a spectral function accounting for the presence of the piled layers in the longitudinal direction.

Using the Galerkin procedure, the same set of functions as the one used for the basis functions is chosen. This way, the original coupled system of IE is transformed into an algebraic linear system of equations, with coefficients α_{Qk} as unknowns

$$\begin{bmatrix} [R_{EE}] & [R_{EH}] \\ [R_{HE}] & [R_{HH}] \end{bmatrix} \begin{bmatrix} [\alpha_E] \\ [\alpha_H] \end{bmatrix} = \begin{bmatrix} [\gamma_E] \\ [\gamma_H] \end{bmatrix}. \quad (3)$$

The term (k, l) in each submatrix (also called reaction term) can be written, using (2), in a condensed form as

$$R_{PQ}(k, l) = \sum_i \tilde{G}_{P_i} C_P(k, i) C_Q^*(l, i), \quad (4)$$

where

$$C_P(k, i) = \int_{D_k} \mathbf{f}_{Pk}(x, y) \mathbf{p}_i(x, y) dx dy. \quad (5)$$

The reaction formula in (4) separates the source and observer contributions in each term of the series expansion. The k th and l th basis functions are projected on each i th modal function using the *overlapping* or *coupling* integral (5).

3. OVERLAPPING INTEGRALS

Considering the overlapping between electric/magnetic sources and TE/TM/TEM modes, there are 6 different combinations of (5) to be solved, namely

$$C_e^\tau = \int_D \mathbf{f} \cdot \mathbf{e}_t^\tau dS \quad (6a)$$

$$C_h^\tau = \int_D \mathbf{f} \cdot \mathbf{h}_t^\tau dS, \quad (6b)$$

with $\tau = \{\text{TE, TM, TEM}\}$. The electric (magnetic) overlapping includes the transversal electric (magnetic) vector component of a mode, as defined in Table 1, and a generic basis function satisfying

$$\nabla_t \times \mathbf{f} = 0 \quad (7a)$$

$$\nabla_t \cdot \mathbf{f} = d \quad (7b)$$

with d a real constant and $\nabla_t = \nabla - \hat{z}\partial/\partial z$.

[1/m]	\mathbf{e}_t	\mathbf{h}_t
TE _{mn}	$\hat{z} \times \nabla_t \chi_{mn} / \kappa_{mn}$	$-\nabla_t \chi_{mn} / \kappa_{mn}$
TM _{mn}	$-\nabla_t \chi_{mn} / \kappa_{mn}$	$-\hat{z} \times \nabla_t \chi_{mn} / \kappa_{mn}$
TEM _m	$-\nabla_t \chi_m^0$	$-\hat{z} \times \nabla_t \chi_m^0$

Table 1. Modal transverse vector components expressed in terms of potential functions χ, χ^0 satisfying Helmholtz and Laplace equations in Ω , respectively.

3.1. Transformation to Contour Integrals

Substituting the field expressions of Table 1 into (6) shows that the initially six combinations can be reduced to only *three* surface integrals

$$\begin{aligned} \int_D \mathbf{f} \cdot (\hat{z} \times \nabla_t \chi) dS &= \int_D (\mathbf{f} \times \hat{z}) \cdot \nabla_t \chi dS = \\ \kappa C_e^{\text{TE}} &= -\kappa C_h^{\text{TM}} = -C_h^{\text{TEM}} \quad (\text{with } \chi = \chi^0) \end{aligned} \quad (8a)$$

$$\int_D \mathbf{f} \cdot \nabla_t \chi dS = -\kappa C_e^{\text{TM}} = -\kappa C_h^{\text{TE}}, \quad (8b)$$

where $\kappa \neq 0$. In the TEM case we also find

$$\int_{\mathbf{D}} \mathbf{f} \cdot \nabla_t \chi^0 dS = -C_e^{\text{TEM}}, \quad (8c)$$

for $\kappa = 0$.

But these expressions can be further simplified if the surface integrals are transformed into contour integrals. This is mainly achieved, after some mathematical manipulations, by using the Green's first identity

$$\int_{\mathbf{D}} \mathbf{A} \cdot \nabla_t B dS = \oint_{\partial \mathbf{D}} B \hat{\nu} \cdot \mathbf{A} dl - \int_{\mathbf{D}} B \nabla_t \cdot \mathbf{A} dS \quad (9)$$

where $\{\mathbf{A}, \nabla_t B\}$ are two generic vector functions. The vectors $\hat{\nu}, \hat{\tau}$ are defined on the contour $\partial \mathbf{D}$ as can be deduced from Fig. 1. The TEM case also requires the definition of an auxiliary potential function g satisfying

$$\mathbf{f} = \nabla_t g, \quad (10a)$$

$$\Delta_t g = d. \quad (10b)$$

A summary of the equivalent contour integrals is given in Table 2. It should be underlined that at this point the overlapping integrals suffered a considerable simplification by only imposing weak conditions on the basis functions. The basis functions are only evaluated along the normal (subindex ν) or tangential (subindex τ) of the source domain's contour.

Surface integral	Contour integral.
$\int_{\mathbf{D}} \mathbf{f} \cdot (\hat{z} \times \nabla_t \chi) dS$	$\oint_{\partial \mathbf{D}} \chi f_{\tau} dl$
$\int_{\mathbf{D}} \mathbf{f} \cdot \nabla_t \chi dS$	$\oint_{\partial \mathbf{D}} \chi f_{\nu} dl + \frac{d}{\kappa^2} \oint_{\partial \mathbf{D}} \frac{\partial \chi}{\partial \nu} dl$
$\int_{\mathbf{D}} \mathbf{f} \cdot \nabla_t \chi dS$	$\oint_{\partial \mathbf{D}} g \frac{\partial \chi^0}{\partial \nu} dl$

Table 2. Surface to contour integral equivalencies.

3.2. Subsectional Basis Functions on Polygonal Domains

Subsectional basis functions are a convenient and frequent choice in IE-MoM problems specially when the surface sources have arbitrary shapes. Each function is defined over a polygonal support \mathbf{D} (an ensemble of cells) that divides the original planar surface. For this reason, the contour integrals of Table 2, can be expressed as a sum of one-dimensional integrals over each side of the cell

$$\oint_{\partial \mathbf{D}} \cdots = \sum_{q=1}^N \left(\int_{\partial \mathbf{D}_q} \cdots dl \right) = \sum_{q=1}^N L_q \left(\int_0^1 \cdots dt \right). \quad (11)$$

The parametrization used in this case

$$\sigma_q : \begin{matrix} [0, 1] \\ t \end{matrix} \begin{matrix} \longrightarrow \\ \rightsquigarrow \end{matrix} \begin{matrix} \mathbb{R}^2 \\ \mathbf{r}(t) = \mathbf{P}_q + L_q t \hat{\tau}_q. \end{matrix} \quad (12)$$

maps each q th side into the $t \in [0, 1]$ segment. Regarding Fig. 1, each side starts in \mathbf{P}_q and it has a distance L_q in the direction $\hat{\tau}_q$.

Moreover, considering rooftops rectangular cells or RWG basis functions [3] (note that both satisfy (7)) the evaluation of \mathbf{f} components along the cell's edge can be expressed as polynomial functions in the variable t .

The normal component f_{ν} vanishes since, by definition, is zero or the vector direction is always parallel to the edges. The only exception appears if a half-rooftop basis function is defined (e.g. in a δ -gap excitation scheme). In this case, the normal component is set to be constant (normally equal to unity) on the non-vanishing edge, that will be denoted as $\partial \mathbf{D}^C$.

On the other hand, the longitudinal variation f_{τ} along an edge is linear and therefore the function g , defined in (10), must be quadratic in t . More specifically,

$$\mathbf{f}_p(\sigma_q(t)) \cdot \hat{\tau}_q = A_1(p, q)t + A_0(p, q) \quad (13a)$$

$$g_p(\sigma_q(t)) = B_2(p, q)t^2 + B_1(p, q)t + B_0(p, q) \quad (13b)$$

with $A_i(p, q), B_i(p, q) \in \mathbb{R}$ being constants that depend on the q th side and p th orientation of the basis function with respect to the cell.

Therefore, the expressions in Table 2 can be rewritten as

$$\int_{\partial \mathbf{D}_q} \chi \mathbf{f}_p \cdot \hat{\nu}_q dl = \begin{cases} \int_0^1 \chi(\sigma_q(t)) dt, & \text{if } \partial \mathbf{D}_q = \partial \mathbf{D}^C; \\ 0, & \text{otherwise.} \end{cases} \quad (14a)$$

$$\int_{\partial \mathbf{D}_q} \chi \mathbf{f}_p \cdot \hat{\tau}_q dl = L_q \sum_{i=0}^1 A_i(p, q) \int_0^1 t^i \chi(\sigma_q(t)) dt \quad (14b)$$

$$\int_{\partial \mathbf{D}_q} g_p \frac{\partial \chi^0}{\partial \nu_q} dl = L_q \sum_{i=0}^2 B_i(p, q) \int_0^1 t^i \nabla_t \chi(\sigma_q(t)) \cdot \hat{\nu}_q dt \quad (14c)$$

$$\int_{\partial \mathbf{D}_q} \frac{\partial \chi}{\partial \nu_q} dl = L_q \int_0^1 \nabla_t \chi(\sigma_q(t)) \cdot \hat{\nu}_q dt. \quad (14d)$$

Regarding (14), the integral problem is now reduced to the solution of only *two* types of one-dimension integrals in $t \in [0, 1]$ on each q th segment of the polygon, namely

$$\int_0^1 t^i \chi(\sigma_q(t)) dt, \quad (15a)$$

and

$$\int_0^1 t^i \nabla_t \chi(\sigma_q(t)) \cdot \hat{\nu}_q dt. \quad (15b)$$

for $i = 0, 1, 2$.

3.3. Boundary Conditions

It is evident from (15), that solving the problem for a different lateral BC is achieved by *simply* using the corresponding potential function χ . Moreover, the resulting integrals have analytic solution for most of the known shapes with PEC/PMC or periodic boundary conditions (PBC).

For example, if the structure is confined into a rectangular waveguide (PEC with rectangular shape $a \times b$) then the potential functions are trigonometric functions defined as $\chi(x, y) = \{\phi, \psi\}$ and $\kappa = k_{mn}$ for TE and TM cases

$$\psi_{mn} = \sqrt{\frac{\epsilon_m \epsilon_n}{\Omega}} \cos(k_m x) \cos(k_n y) \quad (16a)$$

$$\phi_{mn} = \frac{2}{\sqrt{\Omega}} \sin(k_m x) \sin(k_n y) \quad (16b)$$

respectively; with $\Omega = ab$, $\epsilon_n = \begin{cases} 1, & \text{if } n = 0; \\ 2, & \text{if } n \neq 0. \end{cases}$, $k_m = \frac{m\pi}{a}$ and $k_n = \frac{n\pi}{b}$.

On the other hand, a periodic structure (PBC on $\partial\Omega$) consisting in a general skewed lattice (with an angle α) illuminated with a plane wave \mathbf{k}^{inc} defines a potential function $\chi(x, y)$ for each Floquet mode as

$$\chi_{mn} = \frac{1}{\sqrt{\Omega}} \exp \left[j(k_{xm}x + k_{ymn}y) \right],$$

where $\Omega = |\mathbf{a} \times \mathbf{b}| = ab \sin \alpha$, $k_{xm} = \frac{2m\pi}{a} - k_x^i$ and $k_{ymn} = \frac{2n\pi}{b \sin \alpha} - k_y^i \sin \alpha - \frac{2m\pi}{a \tan \alpha}$.

The formulation of other type of boundary conditions is analogous as soon as the eigenmode solution is known.

4. NUMERICAL EXAMPLES

A free-standing strip enclosed using different BC walls, as represented in Fig. 2, will serve as example to show the validity of this unified approach. The strip is subdivided with rectangular cells. The dashed rectangle $\partial\Omega$ surrounding the figure delimits the BC contour.

In the first example, depicted in Fig. 3(a), the strip is used as a planar obstacle inside a rectangular waveguide to scatter the fundamental mode. The response is plotted in Fig. 4. Next, the strip is periodically repeated in an infinite rectangular lattice as shown in Fig. 3(b). The scattering of a linearly polarized plane wave impinging on the structure is given in Fig. 5.

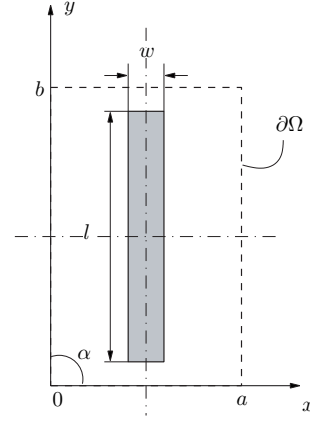


Figure 2. Free-standing strip (solid line) with PEC or periodic boundary conditions (dashed line). Dimensions are in mm: $w = 2.38$, $l = 13.3$, $a = 7.6$, $b = 15.2$.

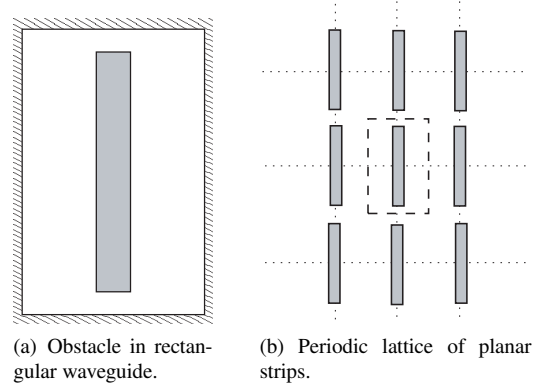


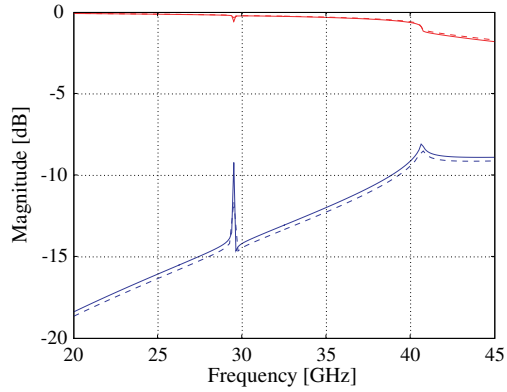
Figure 3. Structure of Fig. 2 represented in with different BCs.

5. CONCLUSIONS

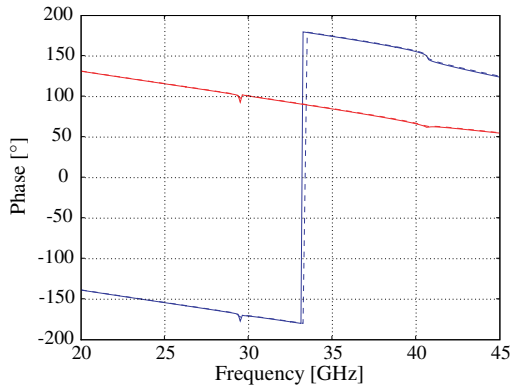
The presented method provides an efficient technique to analyze practical planar structures in multilayered-bounded media. It provides a simple and versatile formulation allowing to deal with different topologies with minor changes. In addition, an analytic solution of the integral expressions is found in most cases, the numerical stability and convergence is easy to check and the computer code needed to implement it is considerably reduced.

ACKNOWLEDGMENT

The authors would like to thank Dr. Daniel Llorens del Rio for his always useful suggestions during the development of the theory and the implementation of the computer algorithms.



(a) Insertion (red) and Return (blue) losses.

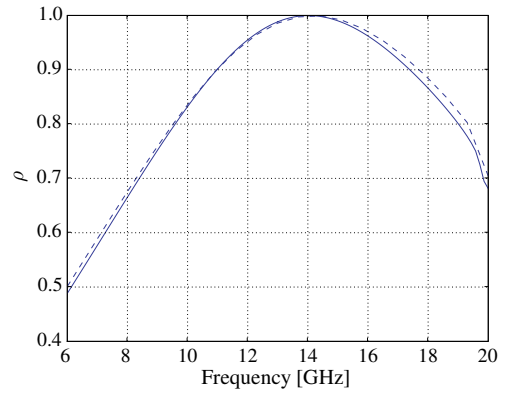


(b) Phase of transmission (red) and reflection (blue) coefficients.

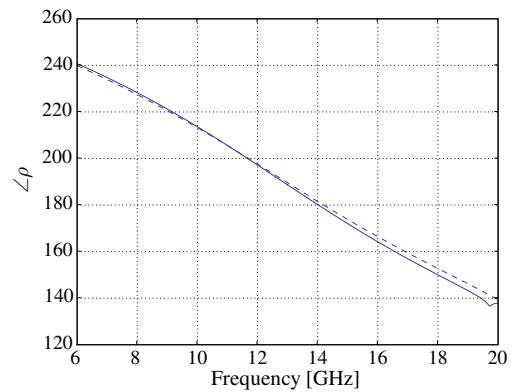
Figure 4. The scattering parameters of the TE_{01} mode. Results obtained using this method are shown in solid lines and the method in [4] with the dashed lines.

REFERENCES

- [1] R. F. Harrington. *Field Computation by Moments Method*. The Macmillan Company, 1968.
- [2] C. A. Balanis. *Advanced Engineering in Electromagnetics*. Wiley, New York, 1989.
- [3] S. Rao, D. Wilton, and A. Glisson. Electromagnetic scattering by surfaces of arbitrary shape. *IEEE Transactions on Antennas and Propagation*, 30:409–418, May 1982.
- [4] I. Stevanović, P. Crespo-Valero, and J. R. Mosig. An integral-equation technique for solving thick irises in rectangular waveguides. *IEEE Transactions on Microwave Theory and Techniques*, 54(1):189–197, January 2006.
- [5] C. H. Chan and R. Mittra. On the analysis of frequency-selective surfaces using subdomain basis functions. *IEEE Transactions on Antennas and Propagation*, 38(1):40–50, January 1990.



(a) Magnitude of the reflection coefficient.



(b) Phase of the reflection coefficient.

Figure 5. The reflection coefficient as a function of frequency for a TE_{00} illumination with $\theta = 0.1^\circ$, $\phi = 0^\circ$. Results obtained using presented theory are shown in solid lines and the values taken from [5] with the dashed ones.